

Chaotic Feature in the Light Curve of 3C 273

Lei Liu^{*}

Institute of Particle Physics, Huazhong Normal University, Wuhan 430079, China

Received 2006 month day; accepted 2006 month day

Abstract Some nonlinear dynamical techniques, including state-space reconstruction and correlation integral, are used to analyze the light curve of 3C 273. The result is compared with a chaotic model. The similarities between them suggest that there is a low-dimensional chaotic attractor in the light curve of 3C 273.

Key words: galaxies: active — galaxies: individual: 3C 273

1 INTRODUCTION

Since its discovery by Smith and Hoffleit (1963), the light curve of 3C 273 plays an important role to understand the nature of the quasar. Although it has been subjected to extensive analysis, there is no accepted method of extracting the information from the light curve. The divergence in result of analyzing the light curve ranges from multi-periodic behavior (Kunkel 1967; Jurkevich 1971; Sillanpaa et al. 1988; Lin 2001) to a purely random process (Manwell & Simon 1966, 1968; Terrell & Olsen 1970; Fahlman & Ulrych 1975). Whatever does this *seemingly* random light curve tell us? Could this seeming randomness be another kind of behavior other than the multi-periodic behavior or a purely random process?

In 1963, Edward Lorenz published his monumental work entitled *Deterministic Nonperiodic Flow*. In this paper, he found a strange behavior which can appear in the deterministic nonlinear dissipative system. This behavior seems random and unpredictable and is called *Chaos*. Chaotic behavior is not multi-periodic because it has a continuous spectrum. Useful information can not always be extracted from power spectrum of chaotic signal. Chaotic behavior is also not random because it can appear in a completely deterministic system. The concept of *attractor* is often

^{*} E-mail: liuphy@mail.ccnu.edu.cn

used to describe the chaotic behavior. As the dissipative system evolves in time, the trajectory in state space will head for some final region. We call this final region attractor. The attractor may be an ordinary Euclidean object or a fractal (Feder 1988) which has non-integer dimension and often appears in the state space of chaotic system. For many practical systems, we may not know in advance the required degrees of freedom and of course can not measure all the dynamic variables. How can we discern the nature of the attractor from the available experimental data? In 1980, Packard et al. introduced a technique which can be used to reconstruct state-space attractor from the time series data of a *single* dynamical variable. A practical algorithm subsequently introduced by Grassberger and Procaccia (1983) can be used to determine the dimension of the attractor embedded in the new state space. These techniques constitute a useful diagnostic method of chaos in the practical system.

3C 273 may be a complex nonlinear dissipative system. If so, the complex light variation of 3C 273 may be chaotic. Here we use the techniques introduced by Packard et al. and Grassberger et al. to investigate whether there is a chaotic attractor in the light curve of 3C 273. The paper is arranged as follows: in Sect. 2, a brief introduction to the method for diagnosing chaos; in Sect. 3, we apply this method to a chaotic model and 3C 273, and then the results are compared; in Sect. 4, some discussions are given.

2 METHOD OF ANALYSIS

The state-space reconstruction technique (Packard et al. 1980) which is based on the notion that the attractor of a multi-dimensional dissipative system can be often reconstructed by using the time series data of a *single* variable. Since a detailed presentation of this technique is available in many places (see , for example, Hilbron 1994; Abarbanel et al. 1993; Sprott 2003), we just give a brief introduction below. Let X_1, X_2, \dots, X_N be measurements of a physical variable at the times $t_i = t_0 + (i - 1)\Delta t, i = 1, \dots, N$. From this sequence one can construct a set of d -dimensional vectors $\mathbf{v}_i, i = 1, \dots, N - (d - 1)T$ of the form

$$\mathbf{v}_i = (X_i, X_{i+T}, X_{i+2T}, \dots, X_{i+(d-1)T}), \quad (1)$$

where T , called the *time delay*, is an integral multiple of Δt . We assume that the real attractor in the full state space of the system can be reconstructed from the time-delayed vectors \mathbf{v}_i moving in the d -dimensional state space. d is often called *embedding dimension*. This assumption works well when embedding dimension becomes greater than about twice the dimension of the real attractor (Sprott 2003).

The correlation integral (Grassberger & Procaccia 1983; see also Hilbron 1994; Abarbanel et al. 1993; Sprott 2003) can be used to determine the attractor dimension.

We define this to be

$$C(r) = \frac{1}{(N-k)(N-k-1)} \sum_{i=1}^{N-k} \sum_{j=1, j \neq i}^{N-k} \theta(r - |\mathbf{v}_i - \mathbf{v}_j|) \quad (2)$$

where $k = (d-1)T$, and $\theta(x)$ is the Heaviside function,

$$\theta(x) = \begin{cases} 1 & x \geq 0 \\ 0 & x < 0 \end{cases} \quad (3)$$

For the dissipative system, $C(r)$ behaves as a power of r for small r ,

$$C(r) \propto r^D \quad (4)$$

where D is called *correlation dimension*. Strictly speaking, D is not attractor dimension, but very close to it (Grassberger and Procaccia 1983). Thus attractor dimension can be estimated by using the correlation dimension. Note that for large values of r the finite size of the attractor makes $C(r)$ “saturate” at 1 and for small values of r the finite number of data points causes $C(r)$ to be close to zero. Thus, the curve of $\log_{10} C(r)$ versus $\log_{10} r$ is approximately a straight line just in the intermediate region, as in Fig. 1.

What we first do in practice is to compute the correlation dimension D by using Eq. (2) and Eq. (4). As the value of D depends on the delay time T and the embedding dimension d , we then plot D versus d for different values of T , as in Fig. 2. If there is a chaotic attractor, D should be independent of d until d becomes greater than some value defined by d_{sat} . For some special value of T , d_{sat} is about twice the value of saturation correlation dimension D_{sat} , that is the value independent of d (Sprott 2003). Thus the saturation dimension D_{sat} which corresponds with this special value of T is the attractor dimension which we expect to find by using a single time series data.

3 DATA ANALYSIS

First, we apply the method described in Sect. 2 to Lorenz model which was introduced by E. Lorenz (1963) to model convection in the atmosphere. It treats the fluid system (say, the atmosphere) as a fluid layer that is heated at the bottom (due to the sun’s heating the earth’s surface, for example) and cooled at the top. A detailed derivation of the equations of the Lorenz model can also be found in many textbooks (see, for example, Hilbron 1994). Here we just give the result,

$$\begin{aligned} dx/dt &= \sigma(y - x) \\ dy/dt &= -xz + \gamma x - y \\ dz/dt &= xy - bz. \end{aligned}$$

It is important to stress that the Lorenz model introduced here is not treated as a model of 3C 273. We just use it to produce a set of chaotic time series and show what would happen when the method of chaos diagnostics is used to analyze a set of chaotic time series.

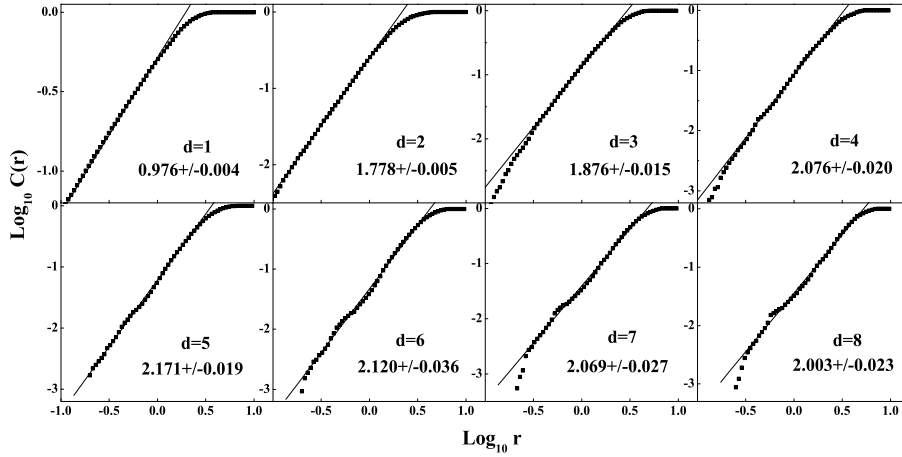


Fig. 1 Correlation integral $C(r)$ of Lorenz model for time delay $T = 20$ and the embedding dimension $d = 1, 2, \dots, 8$ on doubly logarithmic scales. In each panel, the scale of $C(r)$ is arbitrary and the scale of r is same. We also give the slope fitted by using Eq. (4) in each panel.

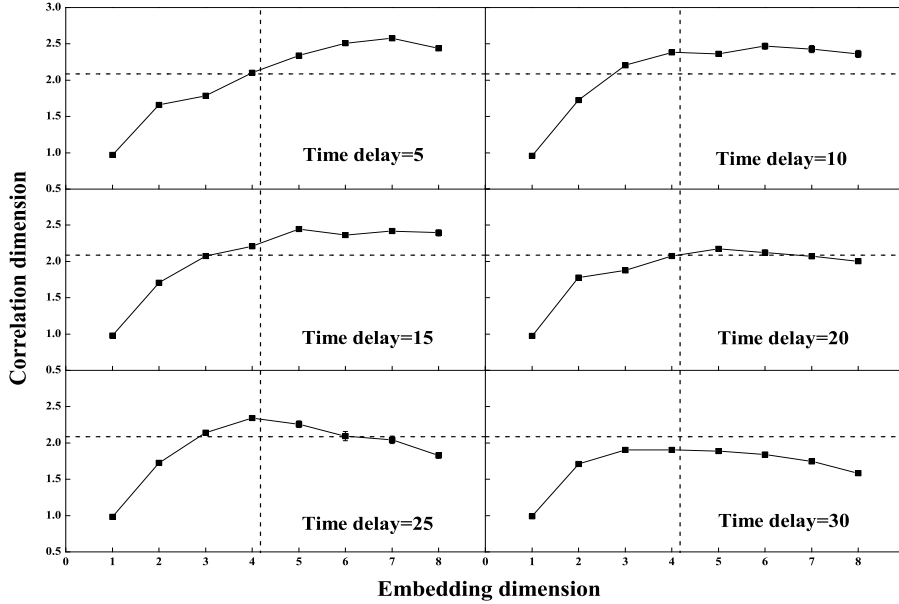


Fig. 2 Correlation dimension D versus the embedding dimension d for Lorenz model. Each panel has the same scale of D and also the same scale of d .

We choose the parameters $\sigma = 10$, $\gamma = 28$ and $b = 8/3$ which are used by many authors to produce a set of chaotic solution of Lorenz equations. We use four-order Runge-Kutta method to solve the equations with the initial conditions $x_0 = 0$, $y_0 = -0.01$, $z_0 = 9$, and generate 292 data points representing $x(t)$ at equally spaced time intervals of $\Delta t = 0.05$. Note that the 292 data points are generated from $t=50$ to assure the trajectory is on the attractor.

The 292 data points are analyzed by using Eq. (2) and Eq. (4). The results of $\log_{10} C(r)$ plotted against $\log_{10} r$ for time delay $T = 20$ are shown in Fig. 1. We can see that in the intermediate region there is a approximately straight line. We also plot $\log_{10} C(r)$ versus $\log_{10} r$ for some other T and find that the curves are also approximately straight lines in the intermediate region as in Fig. 1. The results of correlation dimension D versus embedding dimension d for different time delay T are shown in Fig. 2. Now we carefully compare these curves for different T , and find out that the value of T which makes $d_{sat} \approx 2D_{sat}$ to estimate the attractor dimension. Note that when $T = 25$ and 30, we can't find a good plateau, where D is independent of d , to estimate the attractor dimension. When $T = 5$, the d_{sat} is close to 6. And $D_{sat} \approx 2.508 \pm 0.026$ obtained by averaging the values of correlation dimension for $d = 6, 7, 8$. When $T = 10, 15$ and 20, the d_{sat} is close to 4. And the corresponding $D_{sat} \approx 2.401 \pm 0.039, 2.367 \pm 0.031$ and 2.088 ± 0.025 obtained by averaging D for $d = 4, 5, 6, 7, 8$. Thus the best value which makes $d_{sat} \approx 2D_{sat}$ is 20. The value of D_{sat} estimated from the curve of $T = 20$ is about 2.088 ± 0.025 . Thus, the attractor dimension is about 2.088 ± 0.025 . Two crossing dash lines representing $D_{sat} = 2.088$ and $d_{sat} = 4.176$ are put in Fig. 2. From the two lines, we can not only easily see why $T = 20$ is the special value which we choose to estimate the attractor dimension but also find that there is a downward trend in the value of D_{sat} as T increases. By using the full state space vectors and a large amount of data, one can find a more accurate value of the correlation dimension of Lorenz chaotic attractor which equals 2.068 ± 0.086 (Sprott 2003). Our result is very close to it.

From the analysis of Lorenz model, we know that the curve of $\log_{10} C(r)$ versus $\log_{10} r$ is approximately a straight line in the intermediate region for the dissipative system with an attractor. Thus the correlation dimension can be estimated from the slope of the straight line. Moreover, for the dissipative system, the correlation dimension D will be independent of embedding dimension d as d increases and some special value of delay time T which makes $d_{sat} \approx 2D_{sat}$ can be found out.

Now we analyze the 292 data points of the light curve of 3C 273 in the form of 100-day means (Kunkel 1967). The results of $\log_{10} C(r)$ plotted against $\log_{10} r$ for time delay $T = 30$ are shown in Fig. 3. The curves are also approximately straight lines in the intermediate region as in Fig. 1. The results of correlation dimension D plotted against d for different time delay T are shown in Fig. 4. As in Fig. 2, when $T = 35$, it is difficult to find a good plateau to estimate the attractor dimension. When $T = 10, 15, 20, 25$ and 30, the d_{sat} is close to 5. And the corresponding $D_{sat} \approx 3.17 \pm 0.05, 2.90 \pm 0.05, 2.86 \pm 0.04, 2.82 \pm 0.04$ and 2.72 ± 0.04 obtained by averaging D for $d = 5, 6, 7$ and 8. Thus the best value which makes $d_{sat} \approx 2D_{sat}$ is 30 and the attractor dimension is estimated to be about 2.72 ± 0.04 . Two crossing dash lines in Fig. 4 represent $D_{sat} = 2.7$ and $d_{sat} = 5.4$. By using the two lines, we also easily find that why $T = 30$ is special and that there is a downward trend in the value of D_{sat} as T increases.

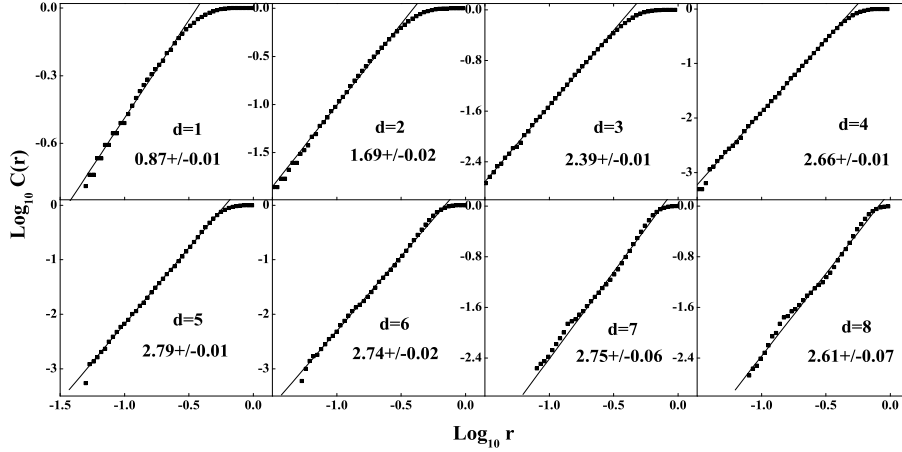


Fig. 3 Correlation integral $C(r)$ of 3C 273 for time delay $T = 30$ and the embedding dimension $d = 1, 2, \dots, 8$ on doubly logarithmic scales. In each panel, the scale of $C(r)$ is arbitrary and the scale of r is same. We also give the slope fitted by using Eq. (4) in each panel.

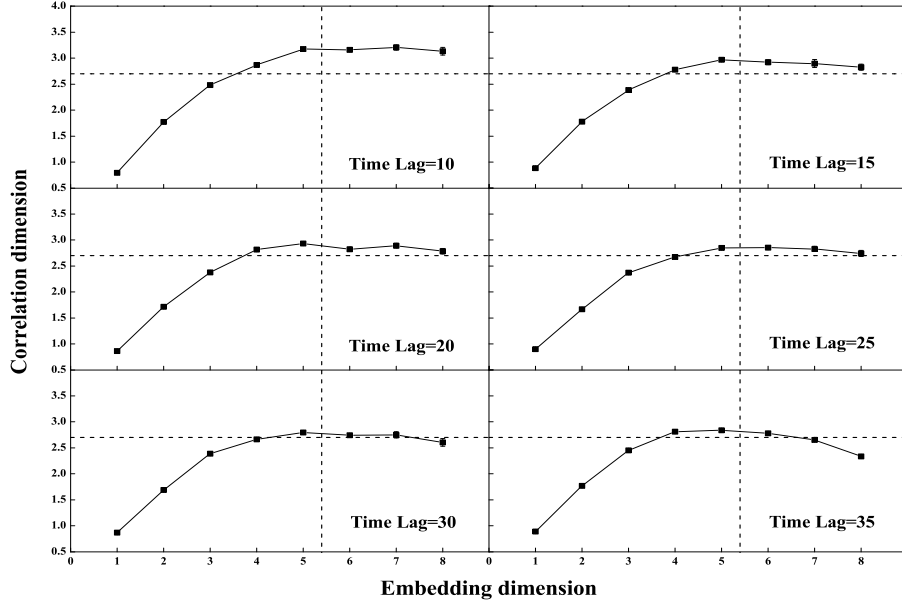


Fig. 4 Correlation dimension D versus the embedding dimension d of 3C 273. Each panel has the same scale of D and also the same scale of d .

At last, we compare Lorenz model with 3C 273. First, the curve of $\log_{10}C(r)$ versus $\log_{10}r$ is approximately a straight line in the intermediate region both in the Lorenz model and 3C 273. Second, the plateau, where the embedding dimension is independent of the correlation dimension, can be found at some values of time delay T both in the Lorenz model and 3C 273. Third, the special time delay T which makes $d_{sat} \approx 2D_{sat}$ can be found out both in the Lorenz model and in the 3C 273. Fourth, there is a downward

trend in the value of D_{sat} as T increases both in the Lorenz model and in the 3C 273. The similarities between them strongly suggest that there is a low-dimensional chaotic attractor in the light curve of 3C 273.

4 DISCUSSION

The nature of AGNs is still an open question. The study of the variation in the light curve of AGNs is expected to yield valuable information about the nature of AGNs. 3C 373 is known as the brightest AGN. In this paper, the state-space reconstruction and correlation integral are used to analyze the light curve of 3C 273. The result is compared with Lorenz model. The similarity between them strongly suggests that there is a low-dimensional chaotic attractor in the light curve of 3C 273. Thus the variation of the light curve of 3C 273 has the nonlinear dynamical origin. It can not be interpreted as multi-periodic behavior or a purely random process. The evidence of chaotic behavior which we show tells that the concepts of nonlinearity may be helpful to understand the nature of the variation in the light curve of AGNs.

It is interesting to compare 3C 273 with other sources. Misra et al. (2004, 2006) have analyzed the X-ray light curves of GRS 1915+105 by using the same method along with surrogate data analysis and find the evidence which is provided for a non-linear limit cycle origin of one of the low frequency QPO detected in the source, while some other types of variability could be due to an underlying low dimensional chaotic system. The chaotic behavior found in the microquasar GRS 1915+105 and the quasar 3C 273 implies that the chaotic behavior may be the universal feature in the seemingly random light curves found in many sources. It is expected to find a common nonlinear dynamical origin to explain this chaotic behavior. This dynamical origin may be the nonlinear temporal evolution of the magneto-hydrodynamic flow of the inner accretion disk (Misra et al. 2004, 2006). It also may come from the turbulent motion in the gaseous cloud around the object (Li & Xiao 2000).

Some authors (Uttley et al. 2005) also consider that the dynamical chaos is not required to explain the data. But our results together with Misra R. et al. cogently prove that the seemingly random light curves found in some sources are indeed chaotic. We expect that our results are confirmed further by using other chaotic and nonlinear time-series analysis.

Acknowledgements I would like to thank Professor Meng Ta-chung for his contribution to my knowledge of nonlinear dynamics. I would also like to thank Wang Xiao-Dong and Yu Yun-Wei for their critical readings of the manuscript. At last, I want to give my especial thanks to Professor Wang En-Ke for his enthusiastic help and encouragement.

References

Abarbanel H. D. I., Brown R., Sidorowich J. J. et al., 1993, Rev. Mod. Phys., 65, 1331

- Fahlman G. G., Ulrych T. J., 1975, *ApJ*, 201, 277
- Feder J., 1988, *Fractal*, New York: Plenum
- Grassberger P., Procaccia I., 1983, *Phys. Rev. Lett.*, 50, 346
- Hilbron R. C., 1994, *Chaos and Nonlinear Dynamics*, Oxford: Oxford University Press
- Jurkevich I., 1971, *Ap&SS*, 13, 154
- Kunkel W. E., 1967, *AJ*, 72, 1341
- Lin R.-G., 2001, *Chin. J. Astron. Astrophys. (ChJAA)*, 1, 245
- Lorenz E. N., 1963, *J. Atmos. Sci.*, 20, 130
- Li Z.-W, Xiao X.-H, 2000, *Astrophysics*, Beijing: Higher Education Press
- Manwell T., Simon M., 1966, *Nature*, 212, 1244
- Manwell T., Simon M., 1968, *AJ*, 73, 407
- Misra R., Harikrishnan K. P., Mukhopadhyay B. et al., 2004, *ApJ*, 609, 313
- Misra R., Harikrishnan K. P., Ambika G. et al., 2006, arXiv: astro-ph/0603281
- Packard N. H., Crutchfield J. P., Farmer J. D. et al., 1980, *Phys. Rev. Lett.*, 45, 712
- Sprott J. C., 2003, *Chaos and Time-Series Analysis*, Oxford: Oxford University Press
- Smith H. J., Hoffleit D., 1963, *Nature*, 198, 650
- Sillanpaa A., Haarala S., Korhonen T., 1988, *A&AS*, 72, 347
- Terrell J., Olsen K. H., 1970, *ApJ*, 161, 399
- Uttley P., McHardy I. M., Vaughan S., 2005, *MNRAS*, 359, 345